Autophagy 8:7, 1045–1057; July 2012; © 2012 Landes Bioscience

Compromised autophagy by *MIR30B* benefits the intracellular survival of *Helicobacter pylori*

Bin Tang,[1,3,†] Na Li,[1†] Jiang Gu,[1] Yuan Zhuang,[1] Qian Li,[1] Hai-Guang Wang,[1] Yao Fang,[1] Bo Yu,[1] Jin-Yu Zhang,[1] Qing-Hua Xie,[1] Li Chen,[1] Xue-Jun Jiang,[2] Bin Xiao,[1] Quan-Ming Zou[1,*] and Xu-Hu Mao[1,*]

[1]Department of Clinical Microbiology and Immunology; College of Medical Laboratory Science; Third Military Medical University; Chongqing, China; [2]Biological Resource Center; The Institute of Microbiology; Chinese Academy of Sciences; Beijing, China; [3]Emei Sanatorium of Chengdu Military Region; Emeishan, Sichuan China

[†]These authors contributed equally to this work.

Keywords: *Helicobacter pylori*, *MIR30B*, autophagy, ATG12, BECN1

Abbreviations: *H. pylori*, *Helicobacter pylori*; 3-MA, 3-methyladenine; miRNAs, microRNAs; TEM, transmission electron microscopy; GFP, green fluorescent protein; MAP1LC3B, microtubule-associated protein 1 light chain 3 beta; FACS, flow cytometry; siRNA, small interfering RNA; SQSTM1, sequestosome 1

Helicobacter pylori evade immune responses and achieve persistent colonization in the stomach. However, the mechanism by which *H. pylori* infections persist is not clear. In this study, we showed that *MIR30B* is upregulated during *H. pylori* infection of an AGS cell line and human gastric tissues. Upregulation of *MIR30B* benefited bacterial replication by compromising the process of autophagy during the *H. pylori* infection. As a potential mechanistic explanation for this observation, we demonstrate that *MIR30B* directly targets ATG12 and BECN1, which are important proteins involved in autophagy. These results suggest that compromise of autophagy by *MIR30B* allows intracellular *H. pylori* to evade autophagic clearance, thereby contributing to the persistence of *H. pylori* infections.

Introduction

Helicobacter pylori (*H. pylori*) is a gram-negative bacterium that plays an etiologic role in the development of gastritis, peptic ulceration and gastric adenocarcinoma.[1] About half of the world's population is infected with *H. pylori*, which is able to adapt and reside in the mucus, attach to epithelial cells, evade immune responses, and achieve persistent colonization in the stomach.[2] Although *H. pylori* is generally considered as an extracellular microorganism, a growing body of evidence supports that at least a subset of *H. pylori* has an intraepithelial location and that a minor fraction of *H. pylori* resides inside gastric epithelial cells.[3-5] The intracellular *H. pylori* fraction may represent the site of residence for persistent infection. Autophagy is a response by eukaryotic cells to a number of deleterious stimuli,[6] and it plays a critical role in the regulation of survival of *H. pylori*. Recent studies suggest that autophagy functions as an innate immune response against *H. pylori*, decreasing its survival.[7,8] Additionally, *H. pylori* can induce autophagy in gastric epithelial cells,[5,8,9] but it still multiplies in these cells.[9,10] The mechanism by which *H. pylori* antagonize host autophagy remains to be elucidated.

Single-stranded noncoding RNA molecules of 19–24 nucleotides, known as microRNAs (miRNAs), control gene expression at the post-transcriptional level,[11] and their disruption is associated with human diseases.[12,13] Accumulating evidence has demonstrated that miRNAs not only play a key regulatory role in the innate immune response to pathogens and stimuli,[14-16] but also regulate autophagy.[17-21] Previously, we used a miRNA microarray to detect the expression profiles of cellular miRNAs, and found that the expression level of *MIR30B* was significantly upregulated during *H. pylori* infection.[22] To further explore the potential target proteins of *MIR30B*, we utilized the bioinformatic tool, Targetscan, and found that BECN1 and ATG12 were the main targets.

BECN1 (BCL2 interacting coiled-coil protein) is part of a Class-III PtdIns3K complex that participates in autophagosome formation, mediating the localization of other autophagy proteins to the preautophagosomal membrane.[23] However, BCL2 anti-apoptotic protein inhibits BECN1-dependent autophagy.[24] ATG12 (autophagy-related protein 12) contributes directly to the elongation of phagophores and the maturation of autophagosomes. In the ATG12 conjugation system, ATG12 is activated by ATG7, an E1-like enzyme, transferred to ATG10, an E2-like enzyme, and conjugated to ATG5 to form an ATG12-ATG5 conjugate.[25] This conjugate functions as an E3-ligase complex to facilitate MAP1LC3B lipidation. Thus, BECN1 and ATG12 are both important proteins in regulating autophagy.

*Correspondence to: Xu-Hu Mao and Quan-Ming Zou; Email: mxh95xy@tom.com and qmzou2007@163.com
Submitted: 05/16/11; Revised: 03/22/12; Accepted: 03/26/12
http://dx.doi.org/10.4161/auto.20159

We hypothesized that *MIR30B* could downregulate BECN1 and ATG12 expression to compromise autophagy, resulting in increased *H. pylori* intracellular survival.

Results

Autophagy increases in AGS cell lines during *H. pylori* infection, but decreases in patients with chronic *H. pylori* infection. To determine whether autophagy could be induced during *H. pylori* infection, we investigated the ratio of MAP1LC3B-II to actin, which is considered as an accurate indicator for autophagy.[26,27] We observed that there was a gradual increase over time in the ratio of MAP1LC3B-II to actin with *H. pylori* infection (MOI = 100:1) as compared with an uninfected control. In addition, by measuring SQSTM1 degradation, we observed a gradual decline in SQSTM1 protein levels upon *H. pylori* infection (**Fig. 1A**). Be consistent with the observed MAP1LC3B-II ratios and SQSTM1 degradation in time-course experiments, similar results were

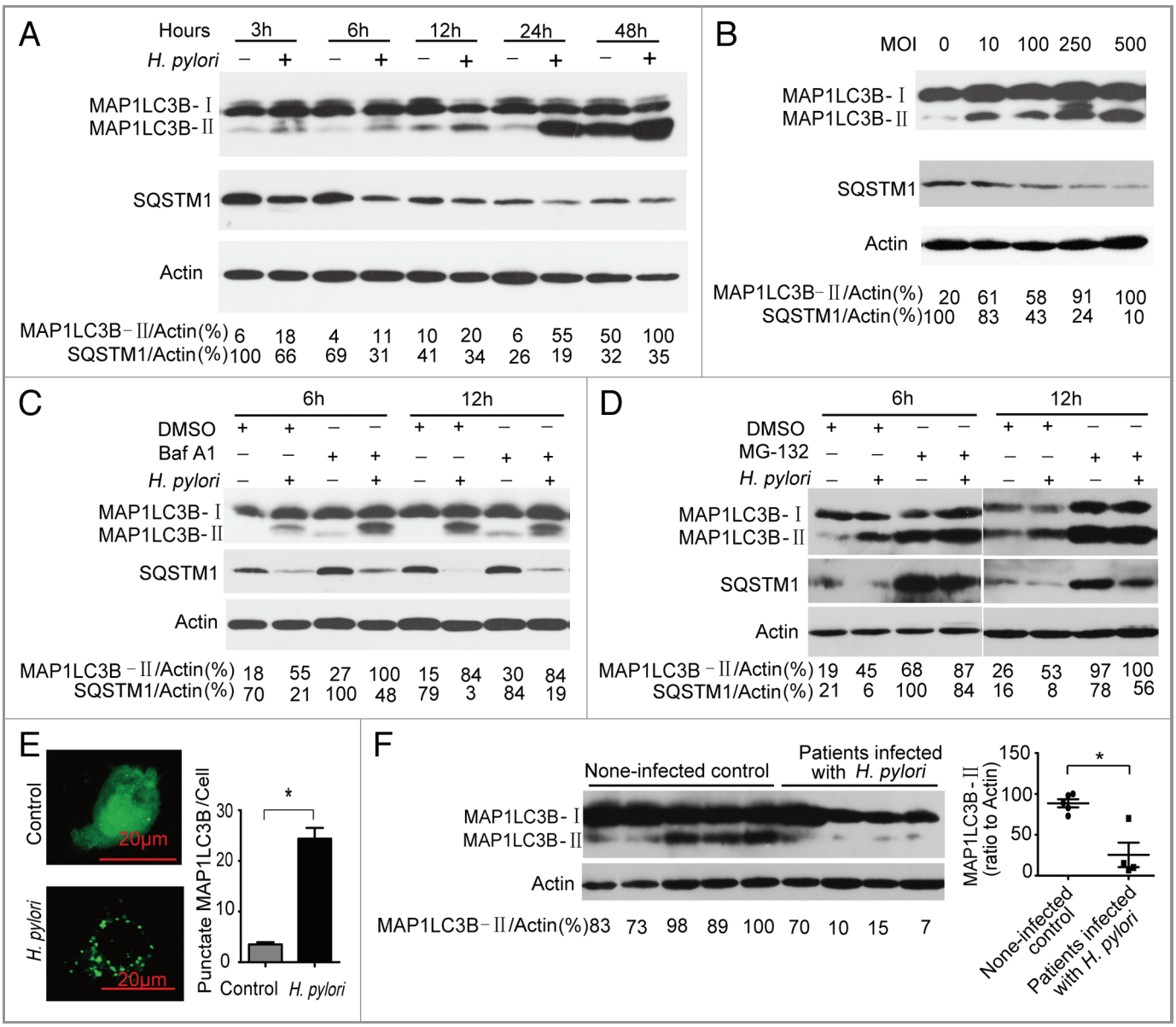

Figure 1. Autophagy is induced after *H. pylori* infection, but it was decreased in patients with chronic *H. pylori* infection. (A and B) *H. pylori* increased the conversion of MAP1LC3B-I to MAP1LC3B-II in AGS cells. AGS cells were treated with *H. pylori* (MOI = 100:1) for 3, 6, 12, 24 and 48 h and treated with *H. pylori* at MOI = 0, 10, 100, 250 and 500 for 6 h. (C) *H. pylori* induced incomplete autophagic flux in AGS cells. AGS cells were treated with *H. pylori* (MOI = 100:1) for 6 h in the presence of Baf A_1 (10 nM). (D) AGS cells were treated with *H. pylori* (MOI = 100:1) for 6 h in the presence of MG-132 (10 μM). (E) AGS cells were transfected with a plasmid expressing GFP-MAP1LC3B. After 24 h, the cells were incubated for 6 h at 37°C in F12 medium with *H. pylori*. Following fixation, cells were immediately visualized by confocal microscopy. The number of GFP-MAP1LC3B puncta in each cell was counted. (F) The conversion of MAP1LC3B-I to MAP1LC3B-II in gastric mucosal tissues from *H. pylori*-positive patients (n = 4) was lower than its expression in *H. pylori*-negative individuals (n = 5). Experiments performed in triplicate showed consistent results. Compared with controls, *$p < 0.05$.

observed when testing dose dependency in AGS and BGC-823 cells (**Fig. 1B**; **Fig. S1**). Furthermore, Baf A_1 challenge resulted in further accumulation of MAP1LC3B-II and SQSTM1 in AGS cells after 6 h of infection (**Fig. 1C**), suggesting that *H. pylori* infection promote cellular autophagic processes. However, the concentration of SQSTM1 remains decreased in the presence of Baf A_1. One possibility is that the concentration of Baf A_1 used did not totally block the degradative step of autophagy. Furthermore, AGS cells were challenged with MG-132 (a proteasome inhibitor). MG-132 challenge resulted in further accumulation of MAP1LC3B-II and SQSTM1 in AGS cells (**Fig. 1D**), suggesting that the proteasome can degrade MAP1LC3B-II and SQSTM1 during *H. pylori* infection, or MG-132 can induce autophagy in AGS cells. To further confirm that *H. pylori* induce autophagy in AGS cells, we used a GFP-MAP1LC3B puncta formation assay for monitoring autophagy. *H. pylori*-infected AGS cells displayed a significant increase in the percentage of cells with autophagosomes (GFP-MAP1LC3B dots) after 6 h compared with mock-infected AGS cells ($p < 0.05$) (**Fig. 1E**). These data indicate that a complete autophagic response is induced in an AGS cell line infected with *H. pylori*.[28]

In view of the fact that the infection of *H. pylori* persists throughout life unless specifically treated,[29] the results from the cell model may not well explain the mechanism of disease. Thus, the conversion of MAP1LC3B-I to MAP1LC3B-II in gastric mucosal tissues from *H. pylori*-positive patients and noninfected individuals was detected. As shown in **Figure 1F**, autophagy decreases in patients with chronic *H. pylori* infection compared with noninfected individuals. The exact molecular mechanism underlying this phenomenon remains to be fully elucidated.

Inhibition of autophagy increases intracellular survival of *H. pylori* in AGS cells. Previous studies indicated that *H. pylori* invaded gastric epithelial cells.[28,30-32] In this study, using transmission electron microscopy (TEM), we showed that *H. pylori* invades AGS cells (**Fig. 2A**). To evaluate the number of live internalized *H. pylori* cells in AGS cells, a gentamicin protection assay was used. The number of colony forming units (CFU) of *H. pylori* after 12 h of infection was increased at least 10-fold compared with 3 h of infection, indicating that internalized *H. pylori* underwent replication; CFU then decreased after 12 h (**Fig. 2B**). To determine whether *H. pylori*-induced autophagy could eliminate intracellular bacteria, the effect of autophagy on intracellular survival of *H. pylori* was examined by exposing the cells to an autophagy inhibitor (3-methyladenine, 3-MA) or autophagy activators (starvation, or Rapamycin). A significant increase in the intracellular *H. pylori* population was observed in AGS cells after inhibition of autophagy (3-MA), and a decrease was also observed with inducers of autophagy (Rapamycin and starvation)(**Fig. 2C**). At all time points during a 72-h experiment, it was observed that the number of intracellular *H. pylori* cells in the 3-MA group was elevated compared with the other groups (**Fig. S2**). These findings

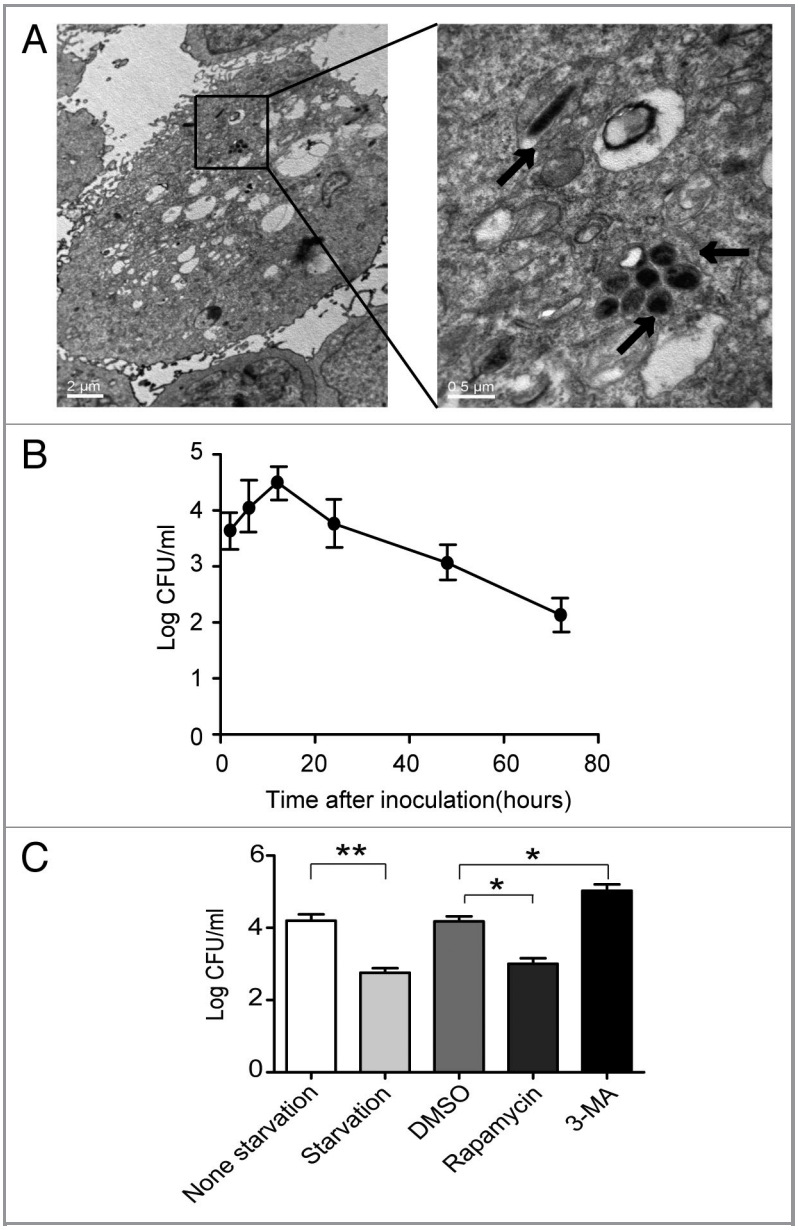

Figure 2. Autophagy inhibition increases multiplication of *H. pylori* in AGS cells. (A) Representative TEM images of AGS cells after 6 h infection with *H. pylori* 26695 (MOI = 100:1). Arrows indicate digested bacteria. (B) Multiplication of *H. pylori* in AGS cells. AGS cells infected with *H. pylori* (MOI = 100:1) for 3, 6, 12, 24, 48 and 72 h were lysed, and intracellular bacteria were quantified after inoculation. The recovered viable *H. pylori* were determined as CFU on a CDC anaerobic blood agar plate. (C) The effects of starvation, 3-MA or rapamycin on the multiplication of *H. pylori* in AGS cells. After pretreatment by starvation, DMSO, rapamycin (100 nM), or 3-MA (2 mM), AGS cells were infected with *H. pylori* 26695 (MOI = 100:1) for 6 h and then lysed. Intracellular bacteria were quantified after inoculation. *$p < 0.05$ by Student's t-test. Results shown are representative of five independent experiments.

indicate that inhibition of autophagy increases the intracellular survival of *H. pylori* in AGS cells.

***MIR30B* is upregulated after *H. pylori* infection.** To confirm the validity of the microarray data, expression of *MIR30B* was examined in gastric mucosal tissues infected with *H. pylori*. A significant increase in *MIR30B* expression was observed in patients infected with *H. pylori* ($p < 0.05$ vs. *H. pylori*–negative persons) (**Fig. 3A**); *MIR30A* was not increased in these samples (**Fig. S3A**). In addition, in gastric epithelial cell lines (AGS, SGC-7901, BGC-823 or HGC-27) infected with *H. pylori* 26695 at different MOI for 6 h, increased expression of *MIR30B* was observed in every cell line but BGC-823 (**Fig. S4**), with AGS cells showing the greatest increase (**Fig. 3B**). We did not find increased expression of *MIR30A* in AGS cell lines (**Fig. S3B**). To monitor the kinetics of *MIR30B* induction, mature *MIR30B* was detected over a period of 72 h following *H. pylori* infection in AGS cells. During *H. pylori* infection, the expression of *MIR30B* rapidly increased from 2 to 12 h of infection, reached the highest levels at 12 h, then decreased slowly from 12–72 h (**Fig. 3C**). Furthermore, there was no effect on expression of *MIR30B* during infection by other pathogens (*E. coli DH5α* and *O157:H7*) or in the presence of autophagy inducer (Rapamycin) and inhibitor (3-MA) (**Fig. S5**). Collectively, the results above suggest that expression of *MIR30B* is increased upon *H. pylori* infection.

***MIR30B* downregulates autophagy after *H. pylori* infection.** To provide evidence that *MIR30B* has a role in the negative regulation of autophagy during *H. pylori* infection, we examined the effect of *MIR30B* on the expression of MAP1LC3B-II and SQSTM1 in AGS cells upon *H. pylori* infection. A *MIR30B* mimic significantly attenuated MAP1LC3B-II conversion and SQSTM1 degradation, while a *MIR30B* inhibitor increased them (**Fig. 4A**). To determine whether the effect of *MIR30B* on autophagy is specific to *H. pylori*, we detected MAP1LC3B-II conversion under starvation conditions. As shown in **Figure S6**, *MIR30B* compromised autophagy in the presence of starvation. Furthermore, co-transfection of a GFP-MAP1LC3B vector and a *MIR30B* mimic significantly decreased formation of GFP-MAP1LC3B dots in AGS cells upon *H. pylori* infection (**Fig. 4B**). TEM of AGS cells transfected with *MIR30B* mimic revealed a decrease in the number of autophagosomes and autolysosomes after 12 h of infection with *H. pylori*, and there were numerous large vacuoles induced by *H. pylori* VacA in the *MIR30B* mimic group but not in the control groups. In the *MIR30B* inhibitor group, the onion-like structure of

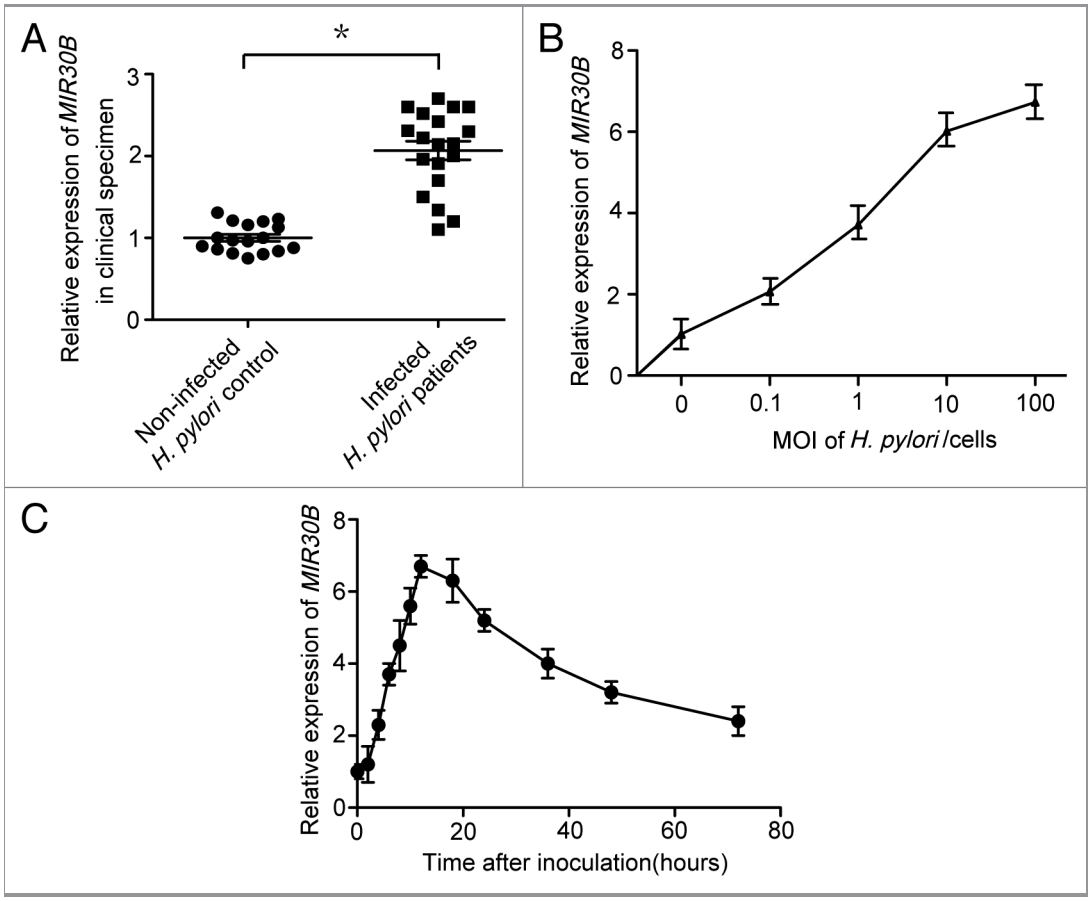

Figure 3. *MIR30B* is upregulated in response to *H. pylori* infection. (A) Expression of *MIR30B* in gastric mucosal tissues from *H. pylori*-positive patients (n = 19) was higher than its expression in *H. pylori*-negative, healthy individuals (n = 17). (B) Real-time PCR detection of *MIR30B* at indicated MOI after infection of AGS cell lines with *H. pylori* for 12 h. (C) The kinetics of *MIR30B* induction assayed by qRT-PCR at different time points (0, 2, 4, 6, 8, 10, 12, 18, 24, 36, 48 and 72 h) after *H. pylori* stimulation of AGS cells (MOI = 100). Data are representative of five independent experiments. *$p < 0.05$ via Student's t-test.

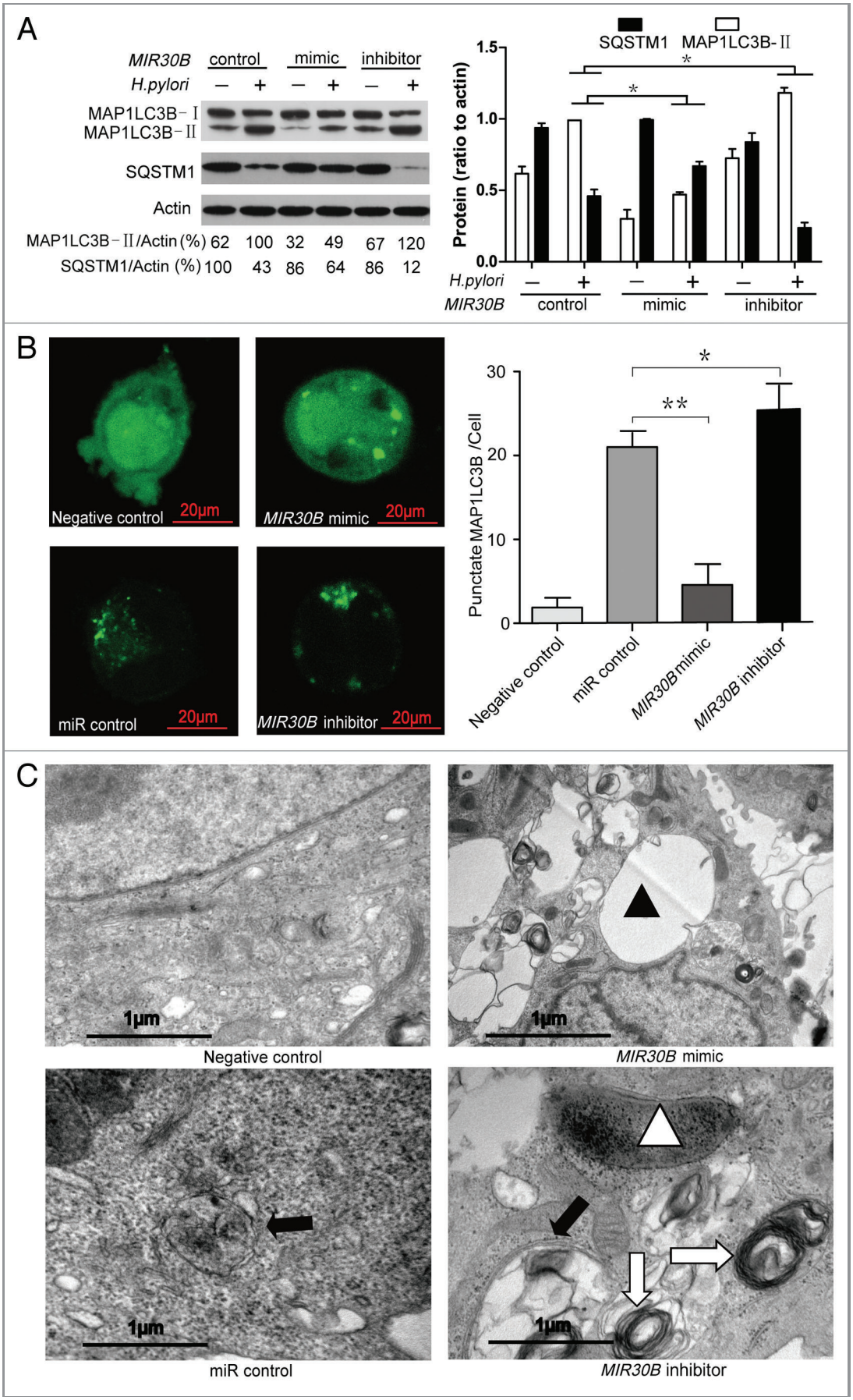

Figure 4. *MIR30B* down-regulates autophagy in *H. pylori* infection. (A) Measurement of MAP1LC3B-II conversion and SQSTM1 degradation with overexpression of *MIR30B* by western blot assay. AGS cells were transfected with *MIR30B* control (100 nM), mimic (100 nM) or inhibitor (100 nM) for 24 h and infected with *H. pylori* for an additional 24 h. Cell lysates were prepared and analyzed. (B) Quantification of GFP-MAP1LC3B puncta (autophagosomes). AGS cells were co-transfected with GFP-MAP1LC3B plasmid and *MIR30B* control, mimic or inhibitor for 24 h, and were then infected with *H. pylori* for an additional 6 h. The number of punctate GFP-MAP1LC3B spots in each cell was counted. (C) Ultrastructural alterations in *H. pylori*-infected AGS cells after transfection with *MIR30B* control, mimic or inhibitor for 24 h. Infected cells were collected for TEM examination. Negative control shows the mock samples without *H. pylori* infection. Closed triangles indicate VacA-dependent large vacuoles whereas open triangles show digested bacteria. Closed arrow indicates autophagosomes whereas open arrow shows the multilayer vesicular structure. The asterisks denote significant differences from control (*$p < 0.05$, **$p < 0.01$). Experiments performed in triplicate showed consistent results.

multiple-layer vesicles, which are recognized as an indicator of enhanced autophagy,[8] was observed more often than in the other groups (**Fig. 4C**). To examine whether VacA-dependent vacuoles are dependent on *MIR30B*, we examined the vacuoles in *H. pylori*-infected cells after transfection of *MIR30B* control, mimic or inhibitor. As shown in **Figure S7**, *MIR30B* mimic increased the number of VacA-dependent vacuoles in *H. pylori*-infected cells. These data indicate that *MIR30B* compromises autophagy during *H. pylori* infection and leads to formation of VacA-dependent large vacuoles.

***ATG12* and *BECN1* are novel targets of *MIR30B*.** In a screen for *MIR30B* targets, *ATG12* and *BECN1* were identified as putative *MIR30B* target genes by using TargetScan (version 4.2, www.targetscan.org) (**Fig. 5A**). To directly address whether *MIR30B* binds to the 3'UTR of target mRNAs, we generated two GFP reporter vectors containing the putative *MIR30B* binding sites within the 3'UTRs of *ATG12* and *BECN1*. GFP fluorescence was significantly reduced in cells co-transfected with *MIR30B* mimic and binding site-containing GFP reporter vectors, while no obvious reduction of GFP fluorescence was observed in cells transfected with miR control or with GFP reporters lacking binding sites (**Fig. 5B**). Similar results were also observed with flow cytometry (**Fig. 5C and Fig. S8**). Furthermore, two luciferase reporter vectors were generated that contain the putative *MIR30B* binding sites within their 3'UTRs. Consistent with the GFP reporter results, the relative luciferase activity was reduced by 70% (3'UTR of *ATG12*) or 40% (3'UTR of *BECN1*) following co-transfection with the *MIR30B* mimic compared with co-transfection with the miR control. In contrast, no change in luciferase activity was observed in cells transfected with reporters lacking binding sites or with the miR control (**Fig. 5D**). The above results suggest that *MIR30B* targets the predicted site in the *ATG12* and *BECN1* genes. To validate the functional inhibition of the two target genes by *MIR30B*, a *MIR30B* mimic was transfected into AGS cells, and subsequently the production of the two proteins was detected by western blot. We observed that the production of the two proteins was decreased with the *MIR30B* mimic as compared with the miR control or mock transfection (**Fig. 5E**). Because miRNAs may downregulate their target genes through mRNA degradation or translation inhibition, we tried to determine which mechanism is responsible for suppression of the two genes by *MIR30B*. We measured the mRNA levels of each gene in AGS cells transfected with the *MIR30B* control, mimic, or inhibitor. Consistent with the western blot results, the mRNA levels of the two genes showed a 50% reduction with the *MIR30B* mimic (**Fig. 5F**). Thus, *MIR30B* may downregulate *ATG12* and *BECN1* expression through mRNA degradation.

Inverse correlation between *MIR30B* and *ATG12*/*BECN1* expression in *H. pylori*-positive human samples. In order to address the biological significance of the interaction between *ATG12*/*BECN1* and *MIR30B* in *H. pylori* infections, we initially examined their expression in the human gastric tissues used in this study. We found that the mRNA levels of *ATG12*/*BECN1* were markedly inhibited in *H. pylori*-positive human samples, compared with normal tissues (**Fig. 6A**). We speculated that the reduced *ATG12*/*BECN1* expression in human samples could be a result of elevated *MIR30B* expression. Therefore, Spearman correlation analysis was used to compare the relative expression levels of *ATG12*/*BECN1* and *MIR30B* in human clinical specimens. We obtained two statistically significant inverse correlations from a total of 19 *H. pylori*-positive gastric tissues (*ATG12*/*MIR30B*, R = -0.886, p = 0.008; *BECN1*/*MIR30B*, R = -0.771, p = 0.01) (**Fig. 6B**), indicating that *MIR30B* expression is inversely correlated with *ATG12*/*BECN1* in human samples.

***MIR30B* increases the intracellular survival of *H. pylori*.** We used siRNAs of target genes and the *MIR30B* mimic to measure the intracellular *H. pylori* survival ratio in AGS cells after 6 h infection. We found that the mRNA and protein levels of *ATG12* and *BECN1* were significantly decreased in AGS cells transfected with siRNAs (**Fig. 7A** and **7B**). Furthermore, *ATG12* and *BECN1* silencing resulted in drastically increased intracellular survival of *H. pylori* in AGS cells ($p < 0.05$, or 0.001 vs. noncoding siRNA control) (**Fig. 7C**). Moreover, we examined intracellular survival of *H. pylori* in AGS cells at different time points after infection in the presence of *MIR30B* control, mimic or inhibitor. After *H. pylori* infection, the intracellular *H. pylori* population rapidly increased, reached its highest level at 12 h, and slowly decreased from 12–72 h (**Fig. 7D**). A similar effect was observed in AGS cells with enforced expression of *MIR30A* (**Fig. S3C**). To further confirm that *MIR30B* can modulate the intracellular survival of *H. pylori*, we detected the effect of *MIR30B* on bacterial survival under autophagy inhibition conditions. As shown in **Figure 7E**, *MIR30B* increased intracellular survival of *H. pylori* in cells treated with 3-MA. Moreover, to obtain further experimental evidence for the possibility, we examined the conversion of MAP1LC3B-I to MAP1LC3B-II with 3-MA and *MIR30B* treatment in *H. pylori* infection, as shown in **Figure S10**. 3-MA (2 mM) could not completely inhibit autophagy. In addition, as shown in **Figure 7F** by confocal microscopy, *H. pylori* resided and multiplied in the cytoplasm, but only a small fraction of them colocalized with autophagosomes. Moreover, there were more intracellular *H. pylori* cells in the *MIR30B* mimic group than in the other treatment groups. Together, these data suggest that *MIR30B* increases the intracellular survival ratio of *H. pylori* in AGS cells.

Figure 5 (See opposite page). *ATG12* and *BECN1* are novel targets of *MIR30B*. (A) The region of the human *ATG12* and *BECN1* mRNA 3′UTR predicted to be targeted by *MIR30B* (TargetScan 4.2). (B and C) Representative fluorescent microscopic image and flow cytometry results demonstrate that GFP expression of the GFP-*ATG12* and *BECN1* reporters was inhibited by *MIR30B*. HEK-293 cells were co-transfected with the GFP reporter vectors and compared with cells transfected with a mimic or control of *MIR30B*. (D) Luciferase reporter assay. HEK293 cells were transiently co-transfected with luciferase reporter vectors and either *MIR30B* mimic or control. Luciferase activity was normalized to the activity of Renilla luciferase. (E and F) AGS cells were transiently transfected with *MIR30B* mimic, inhibitor or control for 24 h. The mRNA and protein levels of *BECN1* and *ATG12* were determined by qRT-PCR and western blot. Data are representative of five independent experiments (*$p < 0.05$).

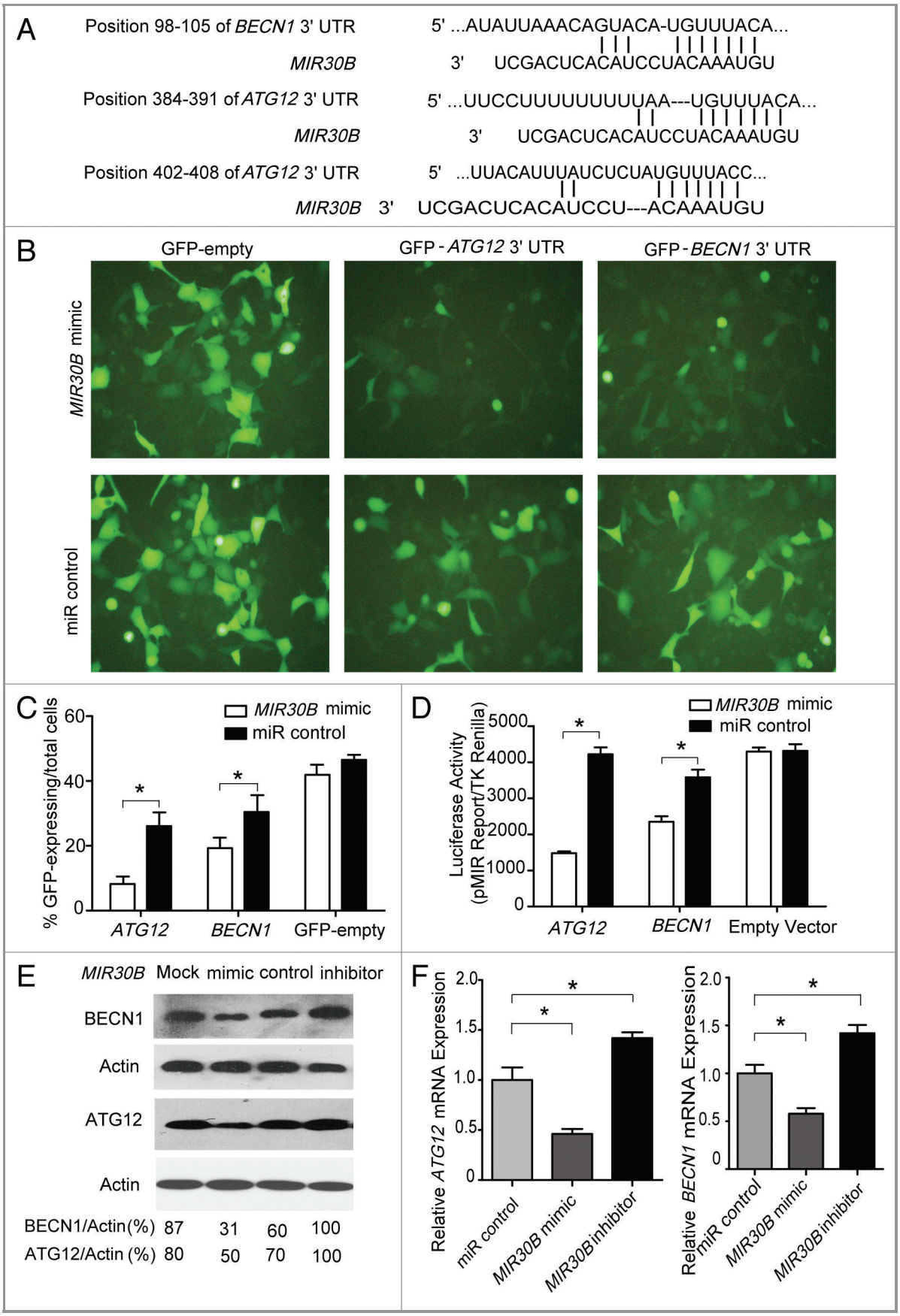

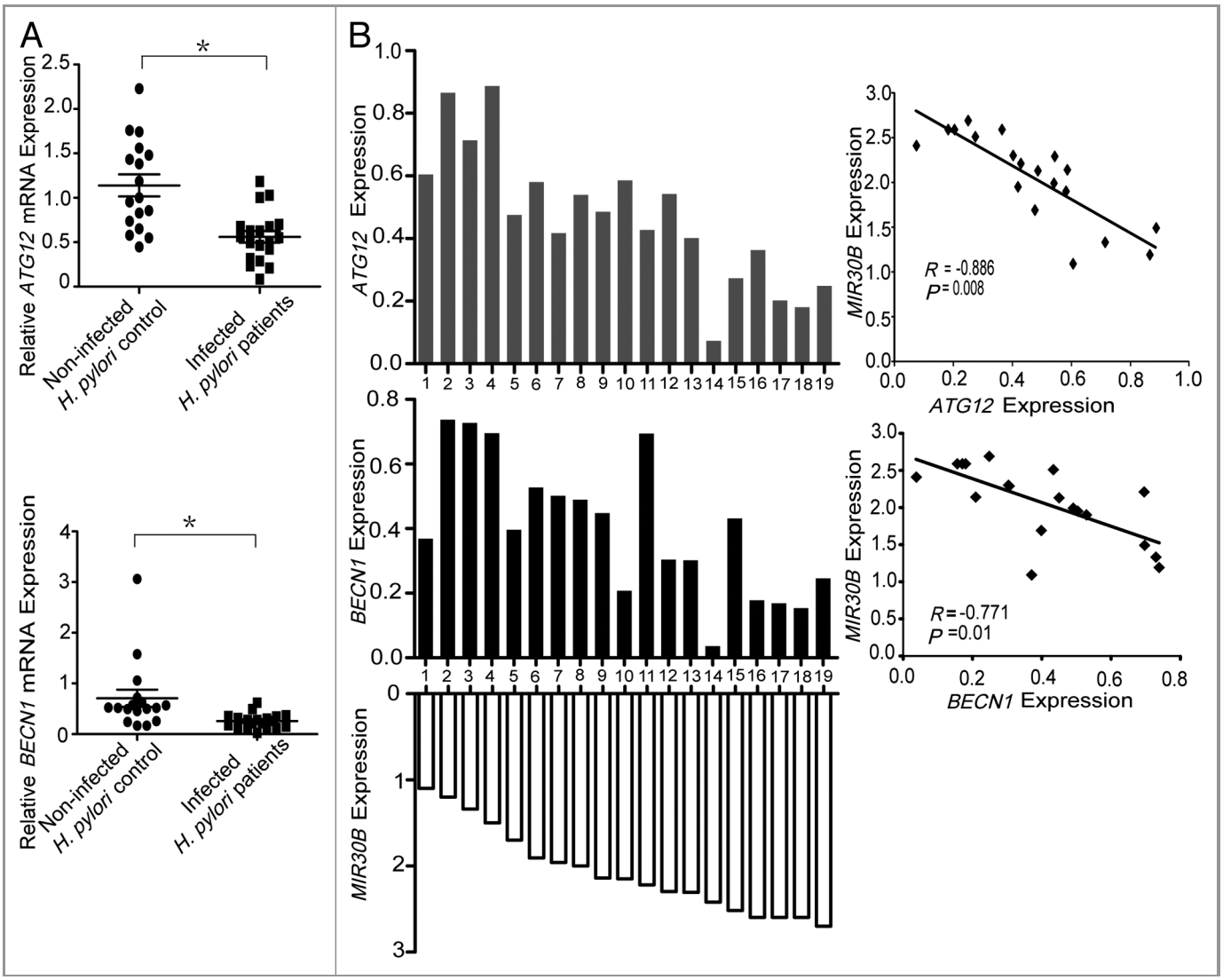

Figure 6. Inverse correlation between *MIR30B* and *BECN1/ATG12* expression in *H. pylori*-positive human samples. (A) *BECN1/ATG12* and *MIR30B* expression levels are inversely correlated in human samples. *BECN1* and *ATG12* mRNA expression in gastric mucosal tissues from *H. pylori*-positive patients (n = 19) were lower than those of *H. pylori*-negative individuals (n = 17). (*p < 0.05) (B) The inverse correlation between *BECN1/ATG12* and *MIR30B* expression levels was examined by Spearman correlation analysis (*BECN1/MIR30B*, *R* = -0.771, p = 0.01; *ATG12/MIR30B*, *R* = -0.886, p = 0.008).

Discussion

Based on the present results, we proposed that compromise of autophagy by *MIR30B* benefits the intracellular *H. pylori* to evade autophagic clearance through targeting *BECN1* and *ATG12*. The novel model is supported by the following data: (1) autophagy decreased in patients with chronic *H. pylori* infection, (2) *MIR30B* was upregulated during *H. pylori* infection in AGS cell line and human gastric tissues, and (3) compromised autophagy by *MIR30B* benefited bacterial replication through targeting *BECN1* and *ATG12* during the *H. pylori* infection.

It is becoming increasingly recognized that altered autophagy is associated with persistent bacterial infection. For example, Yen-Ting Chu et al. have reported that the autophagy inducer rapamycin enhances the clearance of the *H. pylori*.[33] They have also reported that *H. pylori* usurp the autophagic vesicles as the site for replication, and the autolysosomes after fusion will also degrade the replicating bacteria.[33] Therefore, compromised autophagy may benefit the intracellular survival of *H. pylori*. Our findings may provide a novel mechanism for elucidating persistent *H. pylori* infection. The compromised autophagy by *MIR30B* results in a failure to eliminate the intracellular *H. pylori*, leading to persistent infection and proliferation of *H. pylori* in the host cells.

In our study, *H. pylori* infection increased *MIR30B* during in vivo and in vitro infections, but there were inconsistent results of autophagy in the two settings. These different results suggest that *H. pylori*-mediated autophagic processes may be complex.[28] Autophagy plays specific roles in shaping immune system development, fueling host innate and adaptive immune responses, and directly controlling the survival of intracellular microbes as a cell-autonomous innate defense.[34] To resist autophagic clearance, intracellular pathogens have evolved to block autophagic

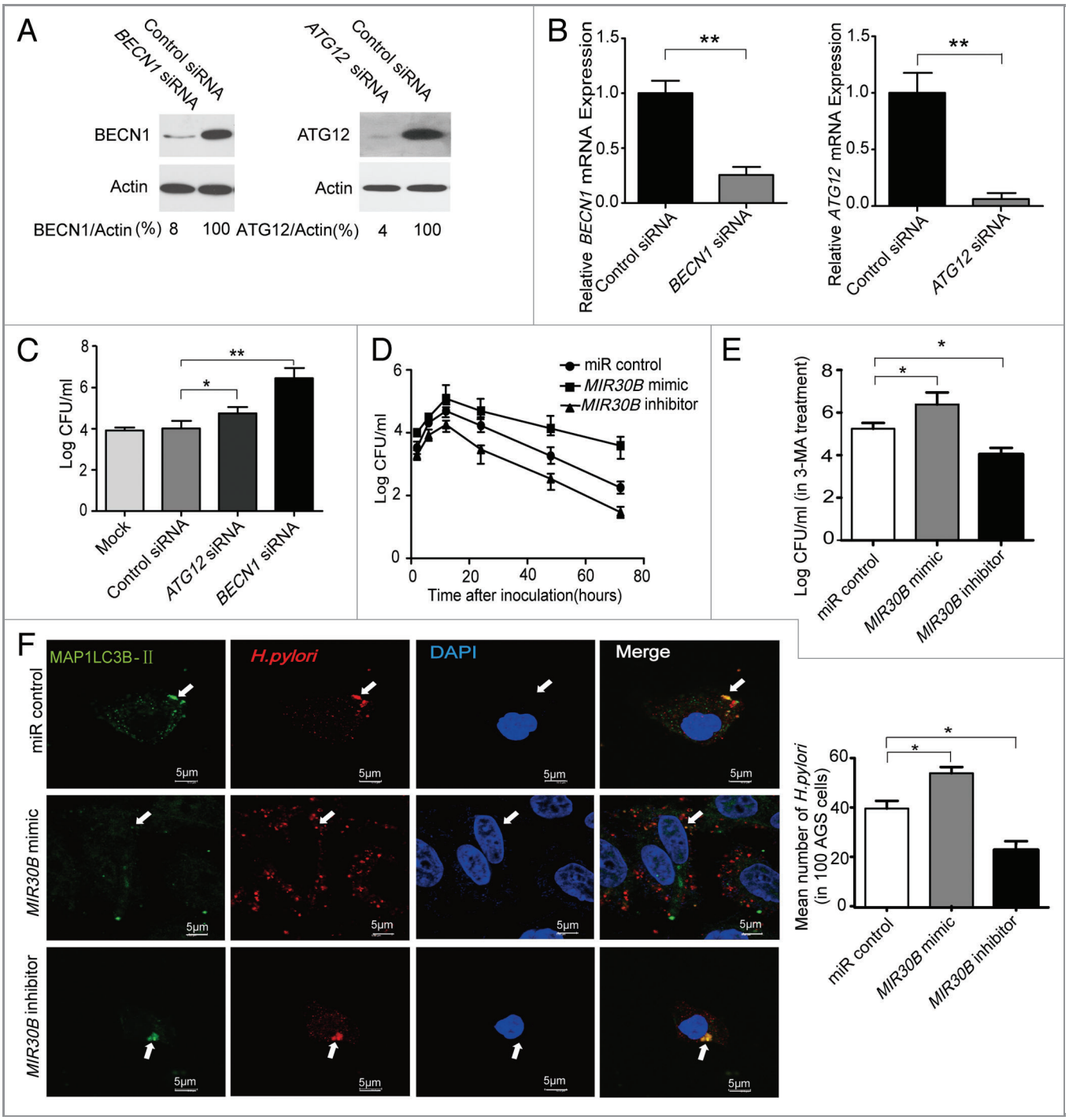

Figure 7. *MIR30B* increases the intracellular survival ratio of *H. pylori*. (A and B) Detection of inhibition efficiency of siRNAs against *BECN1* and *ATG12*. AGS cells were transfected with two siRNAs targeting *BECN1* and *ATG12* (100 nM) for 24 h, and mRNA and protein levels of the two genes were determined by qRT-PCR and western blot. (C) Gentamicin protection assay of the intracellular survival ratio of *H. pylori* with siRNAs against *BECN1* and *ATG12*. AGS cells were transfected with *BECN1*, *ATG12* or a control siRNA at 100 nM for 24 h followed by infection with *H. pylori*. (D) AGS cells were transfected with *MIR30B* control, mimic or inhibitor at 100 nM for 24 h, and were then infected with *H. pylori* for different periods of time (0, 2, 4, 6, 8, 10, 12, 18, 24, 36, 48 and 72 h). Intracellular bacterial counts were determined by gentamicin protection assay. (E) After AGS cells were transfected with *MIR30B* control, mimic or inhibitor, and pretreated by 3-MA for 24 h, intracellular survival of *H. pylori* was detected by gentamicin protection assay. (F) *H. pylori* infection in AGS cells induces GFP-MAP1LC3B puncta formation around the bacteria. AGS cells were transfected by *MIR30B* control, mimic or inhibitor for 24 h, followed by *H. pylori* infection for 6 h. The extracellular bacteria were killed with gentamicin. The infected AGS cells were stained with anti-*H. pylori* antibodies (red) and DAPI (blue). The arrow indicates the presence of *H. pylori* cells. Data are representative of five independent experiments (*$p < 0.05$).

microbicidal defense and subvert host autophagic responses for their survival or growth.[34] In our cell model, although overexpression of *MIR30B* could decrease autophagy through inhibiting the expression of ATG12 and BECN1 (**Fig. 5E**), this adjusting process may lag behind autophagy induced by *H. pylori*. Moreover, the part of downregulated autophagy by *MIR30B* may be not sufficient to block autophagy induced by *H. pylori*. In the study, although *MIR30B* mimic was added exogenously, autophagy in *H. pylori* infection was still more than that in uninfected group (**Fig. 4A**). Thus, in spite of overexpression of *MIR30B*, autophagy still increased during in vitro infection. Given the complexity of *H. pylori* in vivo infection, many factors may be involved in autophagy inhibition. As one of the factors, overexpression of *MIR30B* may slightly continue to compromise the expression of ATG12 and BECN1 for a long time, leading to subverting host autophagic responses for their survival or growth.

It is of note that upon stimulation with *H. pylori* infection, miR-30 family members showed a differential response in which *MIR30B* was upregulated whereas *MIR30A* was not significantly altered. Although miR-30 family members have a similar sequence, they are expressed by genes localized in different chromosomes.[35] It is possible that differential stimuli may affect different genes expression.

Recently, miRNAs have been indicated to play a key role in the regulation of autophagy, such as: *MIR30A*, *MIR17/20/93/106*, *MIR204*, *MIR10B*.[17-19,21] *MIR30A* was reported to regulate autophagy molecule by targeting BECN1.[17] In addition, *MIR17/20/93/106* promote hematopoietic cell expansion by targeting sequestosome 1-regulated pathways in mice,[18] and *MIR204* regulates cardiomyocyte autophagy induced by ischemia-reperfusion through MAP1LC3B-II.[19] In this report, we found that *MIR30B* is a novel regulator of autophagy by targeting BECN1 and ATG12, which are key autophagy-promoting proteins.

To date, about 10 genes have been experimentally validated in predicted targets of *MIR30B*, including *CTGF* (connective tissue growth factor), *UBE2I* (ubiquitin-conjugating enzyme E2I), *ITGB3* (Integrin b3) and *TP53* et al.[35-41] For example, *MIR30B* can interact with 3'UTR of *EED* and regulate endogenous *EED* expression in neural tissues.[42] *LHX1*, a major transcriptional regulator of kidney development, was also targeted by *MIR30B*.[43] Here, we identified *BECN1* and *ATG12*, which are important genes in regulating autophagy, as novel targets of *MIR30B*.

In summary, our findings provide a novel mechanism in which compromised autophagy by *MIR30B* benefits the intracellular survival of *H. pylori*. In addition, these results open a new avenue of research on the potential of miRNAs to modulate autophagy by regulating the expression of key autophagy genes such as *BECN1* and *ATG12*. Although the mechanism of *H. pylori* infection persistence remains to be determined, this study establishes a basis necessary for future evaluation of the role of *MIR30B* in *H. pylori* infections.

Materials and Methods

Antibodies and reagents. The GFP-MAP1LC3B plasmid was kindly provided by Dr. Tamotsu Yoshimori (Department of Cell Biology, National Institute for Basic Biology, Presto, Japan). 3-methyladenine (3-MA, M9281), bafilomycin A_1 (Baf A_1, B1793) rapamycin (Rapa, R8781) and MG-132 (C2211) were purchased from Sigma; antibodies against MAP1LC3B (L7543) and ATG12 (WH0009140m1) were obtained from Sigma. Antibody against BECN1 (612112) was obtained from BD Transduction Laboratories, Inc. whereas antibodies against Actin (sc-10731) and SQSTM1 (sc-28359) were obtained from Santa Cruz Biotechnology.

Cell lines and *H. pylori* strains. Human gastric cancer cell lines AGS and HGC 27 were separately cultured in F12 (Gibco, 11765-054) and DMEM media (Gibco, 11965-092) supplemented with 10% fetal bovine serum (Gibco, 10099-141) and 100 U/ml penicillin/streptomycin (Gibco, 15140-122) in a humidified incubator containing 5% CO_2 at 37°C. The three additional cell lines SGC7901, BGC823 and human embryonic kidney HEK-293 cells were routinely cultured in RPMI 1640 medium (Gibco, 11875-093) supplemented with 10% FBS and penicillin/streptomycin. The wild-type *H. pylori* strain 26695 (700392) was obtained from ATCC and grown as previously described.[44]

Patients and gastric mucosal specimens. In total, 45 patients undergoing gastroscopic examination at Xinqiao Hospital and Southwest Hospital were included in the study. The patients included 23 individuals with *H. pylori*-induced chronic gastritis (median age, 44 y [range, 25–60 y]; 13 women, 10 men) and 22 *H. pylori*-negative control subjects (median age, 32 y [range, 26–55 y]; 14 women, 8 men). The *H. pylori* infection status was confirmed by bacterial culture, C^{13}-urea breath test and histologic testing. Patients were regarded as being *H. pylori*-positive if one or more tests yielded positive results. None of the patients received nonsteroidal anti-inflammatory drugs, and none had taken antibiotics or proton pump inhibitor drugs in the preceding four weeks. The study was approved by the ethics review board at Third Military Medical University, and informed consent was obtained from all patients before participation. Histological assessment was performed according to the Sydney classification by two pathologists who were blinded to the other experimental results.

Plasmid construction. The construction of luciferase reporter vectors and GFP reporter vectors for the *MIR30B* targets *ATG12* and *BECN1* was performed according to the manufacturer's instructions. The 3'UTRs of *BECN1* (439 bp) and *ATG12* (427 bp) were amplified using cDNA from AGS cells (primers for *BECN1*: forward-5'-ACTAGTAGGGGGAGGTTTG-3', reverse-5'-AAAGCTTAGATGTCA-3'; primers for *ATG12*: forward-5'-ACTAGTAACTTGCTACTACA-3', reverse-5'-AAG CTTCA GCCAGCAGGTCAAT-3'), and digested by the SpeI (Takara, D1086) and HindIII (Takara, D1060) restriction enzyme, and ligated into the multiple cloning site of the pMIR-REPORT™ luciferase vector (Ambion, AM5795). The resulting constructs were named pMIR-*BECN1*-wt and pMIR-*ATG12*-wt. To construct a GFP reporter for microRNAs, the luciferase-encoding sequences in the pMIR-REPORT™ vector were replaced with the GFP-encoding sequence from pEGFP-N1 (Clontech, 60851) using BamHI (Takara, D1010) and SpeI restriction sites; the resulting plasmid was named pMIR-GFP-REPORT. The

putative *MIR30B* target sites of *BECN1* and *ATG12* were inserted into the reconstructed GFP reporter vector as described.

Luciferase assay and GFP repression experiments. HEK-293 cells were transfected with 0.8 μg of firefly luciferase reporter vector (pMIR-BECN1-wt or pMIR-ATG12-wt), 100 nM MIR30B mimic (Ambion, 4464066) or control (Ambion, 4464058), and 0.04 μg of Renilla luciferase control vector (pRL-TK-Promega, 2241) using Lipofectamine 2000 (Invitrogen, 11668019). Assays were performed 24 h after transfection using the dual luciferase reporter assay system (Promega, E1910). Firefly luciferase activity was normalized to Renilla luciferase activity. For GFP repression experiments, HEK-293 cells were co-transfected with the indicated MIR30B mimic or control (100 nM) along with pMIR-GFP-BECN1-wt or pMIR-GFP-ATG12-wt. Pictures were taken 24 h after transfection using an Olympus microscope (IX71).

Quantitative RT-PCR. Quantitative RT-PCR (qRT-PCR) analyses for *MIR30A/B* were performed by using TaqMan miRNA assays (Ambion, 4440886) in a Bio-Rad IQ5 (Bio-Rad Laboratories, Inc.). The reactions were performed using the following parameters: 95°C for 2 min followed by 40 cycles of 95°C for 15 sec and 60°C for 30 sec. *RNU6-1* small nuclear RNA was used as an endogenous control for data normalization. Relative expression was calculated using the comparative threshold cycle method. The results represented at least 3 separate experiments performed in triplicate.

Quantitative RT-PCR analyses for the mRNA of *ATG12* and *BECN1* were performed by using PrimeScript RT-PCR kits (Takara, DRR037). The mRNA level of ACTB was used as an internal control. The primer sequences are as follows: *BECN1*, forward-5'-CTGAGGGATGGAAGGGTC-3', reverse-5'-TGGGCTGTGGTAAGTAATG-3'; *ATG12*, forward-5'-AGTAGAGCGAACACGAACCATCC-3', reverse-5'-AAG GAGCAAAGGACTGATTCACATA-3'; ACTB forward-5'-TTCCTTCCTGGGCATGGAGTCC-3', reverse-5'-TGGCGT ACAGGTCT TTGCGG-3'.

siRNA assay. The *ATG12* (human, sc-72578) and *BECN1* siRNAs (human, sc-29797) were purchased from Santa Cruz Biotechnology along with control siRNA (sc-44230). All siRNA transfections were performed with Dharmafect 1 transfection reagent (Thermo Scientific, T-2001-03). AGS cells were transfected with 100 nM siRNA for 48 h, followed by *H. pylori* infection; protein and mRNA knockdown were assessed by western blot analysis and qRT-PCR, respectively.

Transmission electron microscopy. AGS cells were collected and fixed in 2% paraformaldehyde, 0.1% glutaraldehyde in 0.1 M sodium cacodylate for 2 h, postfixed with 1% OsO_4 for 1.5 h, washed and stained for 1 h in 3% aqueous uranyl acetate. The samples were then washed again, dehydrated with graded alcohol and embedded in Epon-Araldite resin (Canemco, 034). Ultrathin sections were cut on a Reichert ultramicrotome, counterstained with 0.3% lead citrate and examined on a Philips EM420 electron microscope.

Confocal microscopy. AGS cells were co-transfected with the indicated *MIR30B* mimics, inhibitors (Ambion, 4464084) or control (100 nM) along with the GFP-MAP1LC3B-expressing plasmid; after 24 h, cells were infected with *H. pylori* for 6 h. After infection, cells were washed with PBS, fixed by incubation for 10 min at 37°C in 4% paraformaldehyde, permeabilized with 0.1% (vol/vol) Triton X-100 and washed with PBS containing 2% BSA. Permeabilized cells were incubated for 1 h with primary antibody at room temperature, washed extensively with PBS buffer, and incubated for 1 h with secondary antibody. All steps were performed at room temperature. The primary antibody used was rabbit anti-*H. pylori* (DAKO, B0471), and the secondary antibody was Alexa Fluor 555-conjugated goat anti-rabbit (Beyotime, P0178). After staining, we mounted coverslips using Vectashield (Vector Laboratories, H1200). We used a Radiance 2000 laser scanning confocal microscope for confocal microscopy followed by analysis with LaserSharp 2000 software (Bio-Rad). We acquired images in sequential scanning mode.

Gentamicin protection assay. After infection, the AGS-bacterium co-culture was washed three times with 1 ml of warm PBS per well to remove nonadherent bacteria. To determine the CFU count corresponding to intracellular bacteria, the AGS cell monolayers were treated with gentamicin (100μg/ml; Sigma, G1272) at 37°C in 5% CO_2 for 1 h, washed three times with warm PBS, and then incubated with 1 ml of 0.5% saponin (Sigma, 47036) in PBS at 37°C for 15 min. The treated monolayers were resuspended thoroughly, diluted and plated on serum agar. To determine the total CFU corresponding to host-associated bacteria, the infected monolayers were incubated with 1 ml of 0.5% saponin in PBS at 37°C for 15 min without prior treatment with gentamicin. The resulting suspensions were diluted and plated as described above. Both the CFU of intracellular bacteria and the total CFU of cell-associated bacteria are given as CFU per well of AGS cells.

Western blot. Cells were washed with ice-cold PBS and then lysed in Triton X-100/glycerol buffer (50 mM TRIS-HCl, 4 mM EDTA, 2 mM EGTA, 1 mM dithiothreitol, and 25% wt/vol sucrose, pH 8.0, supplemented with 1% Triton X-100 and protease inhibitor). After centrifugation at 5,000 × g for 15 min at 4°C, the protein concentration was measured with a BCA protein assay kit (Pierce, 23227). Lysates were separated using SDS-PAGE and transferred to polyvinylidene difluoride membranes. The membranes were blocked with 5% nonfat dry milk in Tris-buffered saline, pH 7.4, containing 0.05% Tween 20 (Sigma, P1379), and were incubated with primary anti-human antibodies and horseradish peroxidase-conjugated secondary anti-mouse antibodies (Jackson Immunoresearch Laboratories, 115-035-003) or anti-rabbit antibodies (Jackson Immunoresearch Laboratories, 111-035-003) according to the manufacturer's instructions. The protein of interest was visualized using Supersignal® West Dura Duration substrate reagent (Thermo, 34080).

Flow cytometry. HEK293 cells were co-transfected with pMIR-GFP-*ATG12* plasmids or pMIR-GFP-*BECN1* plasmids together with *MIR30B* control or mimics. HEK293 cells, used as a blank control, were not transfected. At 24 h post-transfection, cells were subjected to flow cytometric analysis on a FACSCalibur, and data were analyzed with CellQuest software

(both from BD Biosciences). The results presented herein were compiled from three independent experiments.

Statistical analysis. The results are expressed as mean ± SD from at least 3 separate experiments performed in triplicate. The differences between groups were determined with a two-tailed Student's t-test using SPSS 11.5 software. Statistical differences were declared significant at $p < 0.05$. Statistically significant data are indicated by asterisks ($^*p < 0.05$, $^{**}p < 0.01$).

Disclosure of Potential Conflicts of Interest

No potential conflicts of interest were disclosed.

Acknowledgments

We are grateful to Dr. Jiqing Lian, Dr. Fengjun Wang and Zhao Yang for critical reading and editing of the manuscript. We also thank Dr. Tamotsu Yoshimori for providing the GFP-MAP1LC3B plasmid. This study was supported by a grant from National Natural Science Foundation of China (NSFC, No. 81071412).

Supplemental Materials

Supplemental materials may be found here:
www.landesbioscience.com/journals/autophagy/article/20159

References

1. Suerbaum S, Michetti P. Helicobacter pylori infection. N Engl J Med 2002; 347:1175-86; PMID:12374879; http://dx.doi.org/10.1056/NEJMra020542
2. Acheson DW, Luccioli S. Microbial-gut interactions in health and disease. Mucosal immune responses. Best Pract Res Clin Gastroenterol 2004; 18:387-404; PMID:15123077; http://dx.doi.org/10.1016/j.bpg.2003.11.002
3. Petersen AM, Krogfelt KA. Helicobacter pylori: an invading microorganism? A review. FEMS Immunol Med Microbiol 2003; 36:117-26; PMID:12738380; http://dx.doi.org/10.1016/S0928-8244(03)00020-8
4. Wang YH, Wu JJ, Lei HY. When Helicobacter pylori invades and replicates in the cells. Autophagy 2009; 5:540-2; PMID:19270492; http://dx.doi.org/10.4161/auto.5.4.8167
5. Terebiznik MR, Vazquez CL, Torbicki K, Banks D, Wang T, Hong W, et al. Helicobacter pylori VacA toxin promotes bacterial intracellular survival in gastric epithelial cells. Infect Immun 2006; 74:6599-614; PMID:17000720; http://dx.doi.org/10.1128/IAI.01085-06
6. Levine B, Kroemer G. Autophagy in the pathogenesis of disease. Cell 2008; 132:27-42; PMID:18191218; http://dx.doi.org/10.1016/j.cell.2007.12.018
7. Yang JC, Chien CT. A new approach for the prevention and treatment of Helicobacter pylori infection via upregulation of autophagy and downregulation of apoptosis. Autophagy 2009; 5:413-4; PMID:19197143; http://dx.doi.org/10.4161/auto.5.3.7826
8. Wang YH, Wu JJ, Lei HY. The autophagic induction in Helicobacter pylori-infected macrophage. Exp Biol Med (Maywood) 2009; 234:171-80; PMID:19064937; http://dx.doi.org/10.3181/0808-RM-252
9. Wang YH, Gorvel JP, Chu YT, Wu JJ, Lei HY. Helicobacter pylori impairs murine dendritic cell responses to infection. PLoS One 2010; 5:e10844; PMID:20523725; http://dx.doi.org/10.1371/journal.pone.0010844
10. Lei HY, Wang YH, Wu JJ. The Autophagic Induction in Helicobacter pylori-Infected Macrophage. Exp Biol Med 2009; 234:171-80; http://dx.doi.org/10.3181/0808-RM-252
11. Faraoni I, Antonetti FR, Cardone J, Bonmassar E. miR-155 gene: a typical multifunctional microRNA. Biochim Biophys Acta 2009; 1792:497-505; PMID:19268705
12. Eisenberg I, Eran A, Nishino I, Moggio M, Lamperti C, Amato AA, et al. Distinctive patterns of microRNA expression in primary muscular disorders. Proc Natl Acad Sci U S A 2007; 104:17016-21; PMID:17942673; http://dx.doi.org/10.1073/pnas.0708115104
13. Ikeda S, Kong SW, Lu J, Bisping E, Zhang H, Allen PD, et al. Altered microRNA expression in human heart disease. Physiol Genomics 2007; 31:367-73; PMID:17712037; http://dx.doi.org/10.1152/physiolgenomics.00144.2007
14. Taganov KD, Boldin MP, Chang KJ, Baltimore D. NF-kappaB-dependent induction of microRNA miR-146, an inhibitor targeted to signaling proteins of innate immune responses. Proc Natl Acad Sci U S A 2006; 103:12481-6; PMID:16885212; http://dx.doi.org/10.1073/pnas.0605298103
15. Tili E, Michaille JJ, Cimino A, Costinean S, Dumitru CD, Adair B, et al. Modulation of miR-155 and miR-125b levels following lipopolysaccharide/TNF-alpha stimulation and their possible roles in regulating the response to endotoxin shock. J Immunol 2007; 179:5082-9; PMID:17911593
16. Perry MM, Moschos SA, Williams AE, Shepherd NJ, Larner-Svensson HM, Lindsay MA. Rapid changes in microRNA-146a expression negatively regulate the IL-1beta-induced inflammatory response in human lung alveolar epithelial cells. J Immunol 2008; 180:5689-98; PMID:18390754
17. Zhu H, Wu H, Liu X, Li B, Chen Y, Ren X, et al. Regulation of autophagy by a beclin 1-targeted microRNA, miR-30a, in cancer cells. Autophagy 2009; 5:816-23; PMID:19535919
18. Meenhuis A, van Veelen PA, de Looper H, van Boxtel N, van den Berge IJ, Sun SM, et al. MiR-17/20/93/106 promote hematopoietic cell expansion by targeting sequestosome 1-regulated pathways in mice. Blood 2011; 118:916-25; PMID:21628417; http://dx.doi.org/10.1182/blood-2011-02-336487
19. Xiao J, Zhu X, He B, Zhang Y, Kang B, Wang Z, et al. MiR-204 regulates cardiomyocyte autophagy induced by ischemia-reperfusion through LC3-II. J Biomed Sci 2011; 18:35; PMID:21631941; http://dx.doi.org/10.1186/1423-0127-18-35
20. Gabriely G, Teplyuk NM, Krichevsky AM. Context effect: microRNA-10b in cancer cell proliferation, spread and death. Autophagy 2011; 7:1384-6; PMID:21795860; http://dx.doi.org/10.4161/auto.7.11.17371
21. Gabriely G, Teplyuk NM, Krichevsky AM. Context effect: microRNA-10b in cancer cell proliferation, spread and death. Autophagy 2011; 7:1384-6; PMID:21795860; http://dx.doi.org/10.4161/auto.7.11.17371
22. Xiao B, Liu Z, Li BS, Tang B, Li W, Guo G, et al. Induction of microRNA-155 during Helicobacter pylori infection and its negative regulatory role in the inflammatory response. J Infect Dis 2009; 200:916-25; PMID:19650740; http://dx.doi.org/10.1086/605443
23. Kihara A, Kabeya Y, Ohsumi Y, Yoshimori T. Beclin-phosphatidylinositol 3-kinase complex functions at the trans-Golgi network. EMBO Rep 2001; 2:330-5; PMID:11306555; http://dx.doi.org/10.1093/embo-reports/kve061
24. Pattingre S, Tassa A, Qu X, Garuti R, Liang XH, Mizushima N, et al. *Bcl-2* antiapoptotic proteins inhibit Beclin 1-dependent autophagy. Cell 2005; 122:927-39; PMID:16179260; http://dx.doi.org/10.1016/j.cell.2005.07.002
25. Geng J, Klionsky DJ. The Atg8 and *Atg12* ubiquitin-like conjugation systems in macroautophagy. 'Protein modifications: beyond the usual suspects' review series. EMBO Rep 2008; 9:859-64; PMID:18704115; http://dx.doi.org/10.1038/embor.2008.163
26. Klionsky DJ, Cuervo AM, Seglen PO. Methods for monitoring autophagy from yeast to human. Autophagy 2007; 3:181-206; PMID:17224625
27. Mizushima N. Methods for monitoring autophagy. Int J Biochem Cell Biol 2004; 36:2491-502; PMID:15325587; http://dx.doi.org/10.1016/j.biocel.2004.02.005
28. Terebiznik MR, Raju D, Vázquez CL, Torbricki K, Kulkarni R, Blanke SR, et al. Effect of Helicobacter pylori's vacuolating cytotoxin on the autophagy pathway in gastric epithelial cells. Autophagy 2009; 5:370-9; PMID:19164948; http://dx.doi.org/10.4161/auto.5.3.7663
29. Gerrits MM, van Vliet AH, Kuipers EJ, Kusters JG. Helicobacter pylori and antimicrobial resistance: molecular mechanisms and clinical implications. Lancet Infect Dis 2006; 6:699-709; PMID:17067919; http://dx.doi.org/10.1016/S1473-3099(06)70627-2
30. Amieva MR, Salama NR, Tompkins LS, Falkow S. Helicobacter pylori enter and survive within multivesicular vacuoles of epithelial cells. Cell Microbiol 2002; 4:677-90; PMID:12366404; http://dx.doi.org/10.1046/j.1462-5822.2002.00222.x
31. Terebiznik MR, Vazquez CL, Torbicki K, Banks D, Wang T, Hong W, et al. Helicobacter pylori VacA toxin promotes bacterial intracellular survival in gastric epithelial cells. Infect Immun 2006; 74:6599-614; PMID:17000720; http://dx.doi.org/10.1128/IAI.01085-06
32. Necchi V, Candusso ME, Tava F, Luinetti O, Ventura U, Fiocca R, et al. Intracellular, intercellular, and stromal invasion of gastric mucosa, preneoplastic lesions, and cancer by Helicobacter pylori. Gastroenterology 2007; 132:1009-23; PMID:17383424; http://dx.doi.org/10.1053/j.gastro.2007.01.049
33. Chu YT, Wang YH, Wu JJ, Lei HY. Invasion and multiplication of Helicobacter pylori in gastric epithelial cells and implications for antibiotic resistance. Infect Immun 2010; 78:4157-65; PMID:20696835; http://dx.doi.org/10.1128/IAI.00524-10
34. Deretic V, Levine B. Autophagy, immunity, and microbial adaptations. Cell Host Microbe 2009; 5:527-49; PMID:19527881; http://dx.doi.org/10.1016/j.chom.2009.05.016
35. Li J, Donath S, Li Y, Qin D, Prabhakar BS, Li P. miR-30 regulates mitochondrial fission through targeting p53 and the dynamin-related protein-1 pathway. PLoS Genet 2010; 6:e1000795; PMID:20062521; http://dx.doi.org/10.1371/journal.pgen.1000795

36. Martinez I, Cazalla D, Almstead LL, Steitz JA, DiMaio D. miR-29 and miR-30 regulate B-Myb expression during cellular senescence. Proc Natl Acad Sci U S A 2011; 108:522-7; PMID:21187425; http://dx.doi.org/10.1073/pnas.1017346108
37. Zaragosi LE, Wdziekonski B, Brigand KL, Villageois P, Mari B, Waldmann R, et al. Small RNA sequencing reveals miR-642a-3p as a novel adipocyte-specific microRNA and miR-30 as a key regulator of human adipogenesis. Genome Biol 2011; 12:R64; PMID:21767385; http://dx.doi.org/10.1186/gb-2011-12-7-r64
38. Atanackovic D, Hildebrandt Y, Jadczak A, Cao Y, Luetkens T, Meyer S, et al. Cancer-testis antigens MAGE-C1/CT7 and MAGE-A3 promote the survival of multiple myeloma cells. Haematologica 2010; 95:785-93; PMID:20015885; http://dx.doi.org/10.3324/haematol.2009.014464
39. Yu F, Deng H, Yao H, Liu Q, Su F, Song E. Mir-30 reduction maintains self-renewal and inhibits apoptosis in breast tumor-initiating cells. Oncogene 2010; 29:4194-204; PMID:20498642; http://dx.doi.org/10.1038/onc.2010.167
40. Joglekar MV, Patil D, Joglekar VM, Rao GV, Reddy DN, Mitnala S, et al. The miR-30 family microRNAs confer epithelial phenotype to human pancreatic cells. Islets 2009; 1:137-47; PMID:21099261; http://dx.doi.org/10.4161/isl.1.2.9578
41. Duisters RF, Tijsen AJ, Schroen B, Leenders JJ, Lentink V, van der Made I, et al. miR-133 and miR-30 regulate connective tissue growth factor: implications for a role of microRNAs in myocardial matrix remodeling. Circ Res 2009; 104:170-8, 6p, 178; PMID:19096030; http://dx.doi.org/10.1161/CIRCRESAHA.108.182535
42. Song PP, Hu Y, Liu CM, Yan MJ, Song G, Cui Y, et al. Embryonic ectoderm development protein is regulated by microRNAs in human neural tube defects. Am J Obstet Gynecol 2011; 204:544-, e9-17; PMID:21497788; http://dx.doi.org/10.1016/j.ajog.2011.01.045
43. Agrawal R, Tran U, Wessely O. The miR-30 miRNA family regulates Xenopus pronephros development and targets the transcription factor Xlim1/Lhx1. Development 2009; 136:3927-36; PMID:19906860; http://dx.doi.org/10.1242/dev.037432
44. Xiao B, Li W, Guo G, Li B, Liu Z, Jia K, et al. Identification of small noncoding RNAs in Helicobacter pylori by a bioinformatics-based approach. Curr Microbiol 2009; 58:258-63; PMID:19123032; http://dx.doi.org/10.1007/s00284-008-9318-2